ELSEVIER

Catalysis Today 42 (1998) 233–240

CATALYSIS TODAY

Kinetic aspects of the methane oxidative coupling at elevated pressures

Yu.I. Pyatnitsky*, N.I. Ilchenko, M.V. Pavlenko

LV Pisarzhevsky Institute of Physical Chemistry, National Academy of Sciences of Ukraine, 252039 Kiev, Ukraine

Abstract

Computer simulations of the kinetics of the methane oxidative coupling in a plug flow-type reactor at 723–873 K and 0.2–0.6 MPa have been performed. It is shown that the C_2 hydrocarbons and carbon oxides are predominantly formed by the parallel reaction pathways. The heterogeneous catalyst that enables to accelerate the methyl radical formation as well as to decompose the most stable reaction intermediates (CH_2O, H_2O_2 and HO_2) can considerably shift the selectivity and yield of the homogeneous branching chain reaction towards ethane and ethylene formation. The certain accordance between experimental and calculated data indicates this supposed kinetic model to reflect some important features of the heterogeneous–homogeneous methane oxidative coupling under explored reaction conditions. © 1998 Elsevier Science B.V. All rights reserved.

Keywords: Methane; Oxidative coupling; Kinetics; Computer simulation

1. Introduction

Many attempts to find efficient catalysts for the oxidative coupling of methane (OCM) as a means for the conversion of methane to more valuable chemicals were made. The borides, silicides, nitrides and carbides of transition metals are likely to be mentioned among others as potential candidates for efficient catalysts [1,2].

In this report, the kinetics of gas-phase reaction of methane with oxygen at relatively low temperatures (below 873 K) and elevated pressures (>0.1 MPa) is examined. Precisely under these conditions the transition metal compounds with B, Si, and C elements can efficiently catalyze the methane oxidative coupling reaction [3]. These compounds remain largely stable under these catalysis conditions. Indeed, no marked change in the catalyst phase composition and dispersity, owing to the catalysis, has been observed by X-ray and electronic microscopy analyses, and only partial oxidation of the catalyst surface layers has been detected by X-ray spectroscopy [4].

A number of studies on a kinetic modeling of the OCM reaction are known [5–11]. But in spite of this, kinetics of the low-temperature (723–873 K) OCM reaction under elevated pressures (0.2–1 MPa) is not studied enough. In the previously published works, the modeling of the OCM reaction has been performed for significantly different conditions. So far as the rate and selectivity of the OCM reaction are strongly dependent on operating conditions, the modeling of the reaction kinetics at relatively low temperatures and elevated pressures is required for a special study. Thus, such a study has been the subject of the present work.

---

*Corresponding author. Tel.: +380 44 2656645; e-mail: yupyat@ipcp.kiev.ua

0920-5861/98/$32.00 © 1998 Elsevier Science B.V. All rights reserved.
PII S0920-5861(98)00097-2

2. Procedure

2.1. Kinetic measurements

As catalysts, the silicides of titanium, $TiSi_2$ ($0.53\ m^2/g$), and cobalt, $CoSi_2$ ($2.01\ m^2/g$), supplied by Donetsk Chemical Plant, Ukraine, have been explored. The catalyst samples were prepared using pelletized mixtures of powdered silicides and inert material (MgO). The catalyst pellets were of 1–2 mm in size. Experiments were run in a stainless steel flow-type reactor at 723–873 K, 0.1–0.6 MPa, CH_4:O_2:H_2O=48:18:34, utilizing 5–10 g of a catalyst. The residence time defined as the ratio of the free reactor volume to the feed volumetric flow rate was kept constant (approximately 9 s). The reactants (CH_4 and O_2) and reaction products were separated on CaA molecular sieves and 1,2,3-*tris*-β-cyanoethoxy-propane/polysorb A columns.

2.2. Computer simulations

Computer simulations were done using a model consisting of a set of ordinary differential equations of the general form:

$$\frac{dC_j}{dt} = \sum_i r_{ij}^{\text{form}} - \sum_i r_{ij}^{\text{cons}},$$

where C_j is the concentration of component j, r_{ij}^{form} and r_{ij}^{cons}, are the rates of reaction i in which component j is formed and consumed, respectively. The number of the equations corresponds to the number of reaction participants (reagents, products and intermediates).

By way of integration of this set of equations, it is possible to simulate the process carrying out in a perfect plug flow reactor and calculate the concentrations of reaction participants, the rates of elementary reactions, differential and integral selectivities as well as other derivative reaction parameters as functions of residence time.

The contribution analysis was made to simplify a kinetic model by eliminating steps which have little influence on process kinetics. The differential contribution factor of reaction i with respect to component j is defined as a ratio of net rate of a production (consumption) of j, resulting from reaction i, to the net rate of a production (consumption) of j at a given residence time

$$\alpha_{ij} = \frac{v_{ij} r_{ij}}{\sum v_{ij} r_{ij}},$$

where v_{ij} is the stoichiometric coefficient of j in reaction i.

The average lifetimes of the intermediates have been calculated as

$$\tau = \frac{C_i}{\sum r_{ij}^{\text{cons}}}.$$

3. Experimental results

The experimental results are summarized in Table 1. The results show the reagent conversion, selectivities and yield of C_2 hydrocarbons dependencies on the temperature (for $TiSi_2$), and overall pressure (for $CoSi_2$). The data obtained in the absence of the catalyst are also presented. It is shown that the catalysts increase several times as much the conversion of reagents and yield of C_2 hydrocarbons (here, C_2 is defined as a sum of ethane and ethylene). The yield goes through smooth maximum when pressure or temperature is rising. The highest yield has been achieved near 823 K and 0.35 MPa. Thus, in the present work the computer simulations of the reaction kinetics have been made for these conditions used.

4. Computer simulations

4.1. Homogeneous reaction

First, an extended kinetic model of homogeneous reaction was used based on a reaction scheme involving 83 reactions and 21 compounds. The contribution analysis allowed the model to be reduced to 32 elementary reactions. The reduced model is presented in Table 2. The kinetic parameters listed in Table 2 were taken from the database [12], except the reaction CH_3O_2=CH_3+O_2 for which the rate constants (steps (14) and (15) in Table 2) were taken from [13].

An example of calculations for given standard conditions is shown in Fig. 1. The yield of C_2 hydrocarbons for the homogeneous reaction turned out to be

Table 1
Experimental results for the OCM reaction (inlet reaction mixture: 48% CH_4, 18% O_2, 34% H_2O, residence time: 8.7–9.1 s)

Catalyst	T (K)	P (MPa)	Conversion (%)		Selectivity (%)					Y_{C_2} (%)
			CH_4	O_2	C_2H_4	C_2H_6	C_2^+	CO	CO_2	
TiB_2	748	0.36	20.0	55.7	26.6	20.8	47.4	43.7	8.9	9.48
	773	0.35	23.2	61.1	32.4	19.8	52.2	39.2	8.6	12.11
	798	0.35	25.1	65.2	36.2	18.5	54.6	37.7	7.7	13.70
	823	0.34	27.1	70.8	37.0	17.5	54.5	36.4	9.1	14.77
	848	0.35	25.3	71.2	30.9	18.1	49.1	37.3	13.6	12.42
	873	0.35	25.6	74.4	29.5	18.1	47.6	36.7	15.7	12.19
$CoSi_2$	823	0.21	15.0	35.2	29.8	31.2	61.1	33.6	5.4	9.2
	823	0.30	29.6	81.6	34.6	16.1	50.8	35.9	13.4	15.0
	823	0.42	29.2	82.4	34.5	17.1	51.5	34.5	14.0	15.0
	823	0.50	28.4	81.6	36.1	15.8	51.9	32.6	15.5	14.7
	823	0.60	27.3	77.8	33.0	19.6	52.6	30.8	16.6	14.3
No catalyst	798	0.33	9.3	22.7	19.5	32.4	51.9	44.5	3.6	4.83
	823	0.33	11.2	28.2	22.1	29.9	51.1	43.5	5.4	5.72
	873	0.32	14.8	37.8	25.5	24.9	50.5	42.5	7.0	7.47
	923	0.32	22.2	65.1	27.7	16.0	43.8	46.3	9.9	9.72

not too high (maximum value of yield is equal to 3.83% at $x_{CH_4}=19.9\%$ and $S_{C_2}=19.2\%$).

The cause for the low yield is mainly due to the existence of several reactions that lead to complete oxidation of methane to carbon oxides. To understand better the limitations of reaction selectivity, we consider the kinetics of the homogeneous reaction in more detail.

One of the reaction pathways which competes with the CH_3 radical recombination to ethane is the interaction of CH_3 radicals with oxygen by the following scheme:

(14) $CH_3 + O_2 \rightarrow CH_3O_2$

(15) $CH_3O_2 \rightarrow CH_3 + O_2$

(16) $CH_3O_2 + CH_3 \rightarrow 2\,CH_3O$

As calculations show, the reaction CH_3+O_2= CH_3O_2 (steps (14) and (15)) achieves equilibrium very quickly. Then, one may obtain the equation which gives an upper limit of reaction selectivity with respect to C_2 hydrocarbons:

$$S_1 = \frac{2r_2}{2r_2 + 2r_{16}} = \frac{k_2}{k_2 + k_{16}(k_{14}/k_{15})[O_2]}. \qquad (1)$$

At a given oxygen concentration, the S_1 increases when temperature increases (Fig. 2). This is the result of the increase in the rate constant of reaction (15) (the other rate constants in Eq. (1) are slightly dependent on temperature).

Thus, for competition of reaction (2) with reaction (16), the higher temperature is more favorable. However, when the temperature is increased, the role of other reactions with methyl radicals become more important, first of all, the following reaction:

(3) $CH_3 + O_2 \rightarrow CH_3O + O$

This reaction has the great activation energy (approximately 130 kJ/mol). However different from the above considered reactions ((14) and (16)), it leads to the chain branching that may compensate the energy consumption levels. As calculations indicate, reaction (3) is important at the early stage of reaction. Then, the main contribution to the methoxy radical formation is provided by the reaction

(18) $CH_3 + HO_2 \rightarrow CH_3O + OH$

The inequality $r_{18} \gg r_3$ is true for all regions of residence time with the exception of very small time (<1 s). The rate of reaction (18) also exceeds significantly the rate of CH_3 radical consumption via the channel (14)–(16) after that moment when the reagent conversion is not too small (20–200 s).

Table 2
Reduced kinetic model of the homogeneous OCM reaction

No.	Reaction	Rate constant (s^{-1}, m^3/mol s, m^6/mol^2 s)
1	$CH_4+O_2 \to CH_3+HO_2$	4.03×10^7 Exp$(-28640/T)$
2	$2CH_3 \to C_2H_6$	1.01×10^9 $T^{-0.64}$
3	$CH_3+O_2 \to CH_3O+O$	1.99×10^{12} $T^{-1.57}$ Exp$(-14\,710/T)$
4	$CH_3O+M \to CH_2O+H+M$	3.91×10^{31} $T^{-6.65}$ Exp$(-16\,740/T)$
5	$CH_4+H \to CH_3+H_2$	2.25×10^{-2} $T^{3.00}$ Exp$(-4406/T)$
6	$CH_4+O \to CH_3+OH$	1.02×10^3 $T^{1.50}$ Exp$(-4330/T)$
7	$CH_4+OH \to CH_3+H_2O$	1.93×10^{-1} $T^{2.40}$ Exp$(-1060/T)$
8	$CH_3+C_2H_6 \to CH_4+C_2H_5$	5.48×10^{-7} T^4 Exp$(-4169/T)$
9	$C_2H_5+O_2 \to C_2H_4+HO_2$	8.43×10^5 Exp$(-1950/T)$
10	$CH_3+CH_2O \to CH_4+CHO$	5.54×10^{-3} $T^{2.81}$ Exp$(-2950/T)$
11	$CHO+O_2 \to HO_2+CO$	5.12×10^7 Exp$(-850/T)$
12	$CH_4+HO_2 \to H_2O_2+CH_3$	1.81×10^5 Exp$(-9350/T)$
13	$H_2O_2+M \to 2OH+M$	1.29×10^{27} $T^{-4.86}$ Exp$(-26\,795/T)$
14	$CH_3+O_2 \to CH_3O_2$	1.41×10^5
15	$CH_3O_2 \to CH_3+O_2$	5×10^{13} Exp$(-12\,908/T)$
16	$CH_3O_2+CH_3 \to 2CH_3O$	2.41×10^7
17	$H+O_2+M \to HO_2+M$	6.42×10^6 T^{-1}
18	$CH_3+HO_2 \to CH_3O+OH$	1.99×10^7
19	$CO+OH \to H+CO_2$	6.74×10^4 Exp$(0.00091\cdot T)$
20	$C_2H_4+CH_3 \to C_2H_3+CH_4$	3.31×10^{-6} $T^{3.7}$ Exp$(-4780/T)$
21	$C_2H_3+O_2 \to C_2H_2+HO_2$	1.20×10^5
22	$CH_2O+H \to H_2+CHO$	2.19×10^2 $T^{1.77}$ Exp$(-1510/T)$
23	$CO+HO_2 \to OH+CO_2$	1.51×10^8 Exp$(-11\,900/T)$
24	$C_2H_6+OH \to C_2H_5+H_2O$	8.85×10^3 $T^{1.04}$ Exp$(-913/T)$
25	$H+O_2 \to OH+O$	1.69×10^{11} $T^{-0.9}$ Exp$(-8750/T)$
26	$OH+H_2 \to H+H_2O$	$6.38\times T^2$ Exp$(-1490/T)$
27	$2HO_2 \to H_2O_2+O_2$	1.81×10^6
28	$C_2H_6+HO_2 \to H_2O_2+C_2H_5$	2.95×10^5 Exp$(-7520/T)$
29	$CH_2O+O_2 \to HO_2+CHO$	2.05×10^7 Exp$(-19\,600/T)$
30	$CH_2O+OH \to CHO+H_2O$	3.43×10^3 $T^{1.18}$ Exp$(+225/T)$
31	$CH_2O+HO_2 \to H_2O_2+CHO$	1.99×10^6 Exp$(-5870/T)$
32	$CH_3+H_2O_2 \to CH_4+HO_2$	1.20×10^4 Exp$(+300/T)$

The contribution analysis has enabled us to single out the principal pathways of the formation and consumption of the carbon-based species for the homogeneous OCM reaction in the given range of the reaction conditions. The pathways are presented in Fig. 3.

According to the scheme in Fig. 3, selectivity must be affected to a great extent by the ratio of the rate of CH_3 radical recombination to the rate of CH_3 radical interaction with peroxide radicals. With the chain process propagating, as there accumulate HO_2 radicals, the rate of the CH_3+HO_2 reaction comes to prevail over the rate of the $2CH_3 \to C_2H_6$ reaction, which is the reason for the decrease of the selectivity towards C_2-hydrocarbons (Fig. 1).

Outwardly, the pattern of the plummeting selectivity resembles the pattern that could be observed when the reaction ($CH_4 \to C_2 \to CO$, CO_2) proceeds consecutively. However, the contribution analysis indicated that in all stages of chain process C_2-hydrocarbons (including acetylene), and carbon oxides are mostly formed by *parallel* pathways, as shown in the Fig. 3. Sharp decrease of selectivity to C_2 hydrocarbons observed up to 20 s is the result of more higher rate of increase of peroxide radical concentration in comparison with the rate of methyl radical formation.

The main source of peroxide radicals are reactions that are related to the pathway of CH_3 conversion to carbon oxides ($CHO+O_2 \to HO_2+CO$; $CH_3O+M \to CH_2O+M+H$; $H+O_2+M \to HO_2+M$). This branch

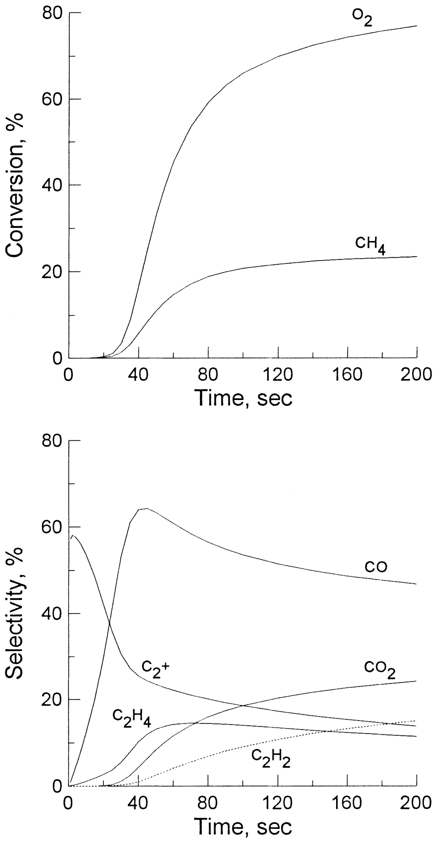

Fig. 1. Simulated conversions of reagents (a) and integral selectivities (b) for the homogeneous OCM reaction as functions of residence time at T=823 K, P=0.35 MPa, 48% CH_4, 18% O_2, 34% H_2O.

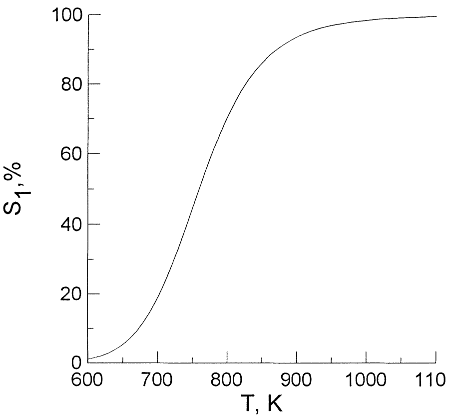

Fig. 2. Upper level of C_2 hydrocarbon selectivity determined by Eq. (1) as function of temperature at 0.35 MPa, 48% CH_4, 18% O_2, 34% H_2O.

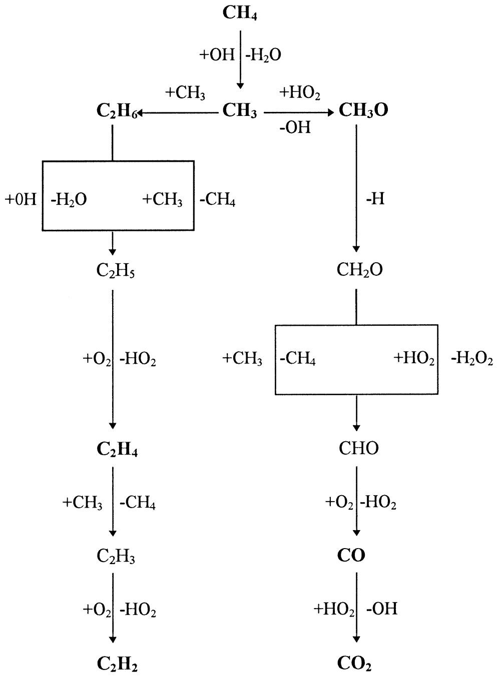

Fig. 3. The main pathways of the conversion of carbon-based compounds.

of the reaction produces the main part of hydrogen peroxide molecules (H_2O_2) and hydrogen peroxide radicals (HO_2). Besides, the reaction CH_4+OH is dominant among other reactions of methane consumption. Therefore, there is the inverse relationship between the total reaction rate and selectivity: when the rate increases, the selectivity to C_2 hydrocarbons decreases.

4.2. *Homogeneous–heterogeneous reaction*

The intermediates of the homogeneous chain reaction can react with the catalyst surface and reactor walls. Then the overall reaction mechanism becomes *heterogeneous–homogeneous*. The probability of the heterogeneous reactions depends on the lifetimes, t_{lt}, of the gas-phase intermediates. With the help of t_{lt}, one can calculate the diffusion path lengths of the intermediates up to the moment when they enter into the reaction using the Einstein–Smoluchowski law of diffusion

$$D = l^2/2 \cdot t_{lt},$$

where D is the diffusion coefficient, and l is the length of the species shift in any direction for the time t_{lt}.

The diffusion path length makes it possible to estimate the likelihood of involvement of the intermediate in the heterogeneous steps. If the path length of a given species is relatively large, then it is highly likely that the species will reach the surface of the catalyst (or the walls of the reactor) without undergoing gas-phase conversion. Such estimations show that the path length of all atoms and radicals with exception of peroxide radical do not exceed 0.001 cm at the given reaction conditions (873 K, 0.35 MPa, 48% CH_4, 18% O_2, 34% H_2O). For HO_2, the average path length is around 0.1 cm, that is comparable with the distance between the catalyst granules. Therefore, we assumed that peroxide radicals can be involving into heterogeneous steps.

Other probable heterogeneous reaction can be a reaction of methane with catalyst producing the methyl radicals as well as the interaction of formaldehyde and hydrogen peroxide molecules with catalyst surface. The mechanism of these reactions is formalized as follows:

(1s) $CH_4 + ZO \rightarrow CH_3^{\bullet} + ZOH$

(1s′) $2\,ZOH \Leftrightarrow Z + ZO + H_2O$

(1s″) $O_2 + 2\,Z \Leftrightarrow 2\,ZO$

(2s) $HO_2 + \text{wall} \rightarrow 1/2\,H_2 + O_2$

(3s) $H_2O_2 + \text{wall} \rightarrow H_2 + O_2$

(4s) $CH_2O + \text{wall} \rightarrow CO + H_2O$

Assuming that the steps (1s′) and (1s″) are in equilibrium and surface coverage by oxygen $\vartheta_{\rm ox}$ is predominant, one may obtain

$$\vartheta_{\rm ox} = \frac{\sqrt{b_{O_2} C_{O_2}}}{1 + \sqrt{b_{O_2} C_{O_2}}}.$$

Then the rate of heterogeneous formation of CH_3 radicals is:

$$r_{1s} = k_{1s} \frac{\sqrt{b_{O_2} C_{O_2}}}{1 + \sqrt{b_{O_2} C_{O_2}}} C_{CH_4} \cdot (S/V),$$

where S/V is the ratio of catalyst surface area to free reactor volume.

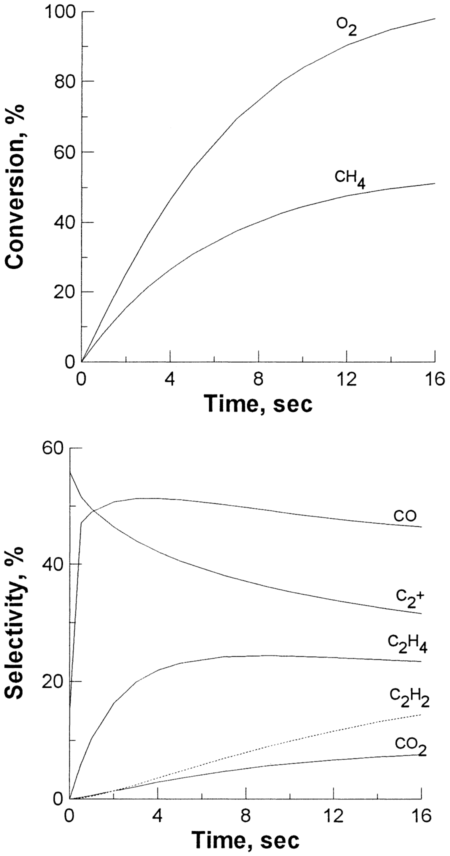

Fig. 4. Simulated conversions of reagents (a) and integral selectivities (b) for the heterogeneous–homogeneous OCM reaction as functions of residence time at T=823 K, P=0.35 MPa, 48% CH_4, 18% O_2, 34% H_2O, $S/V=10^6\,m^{-1}$, $k^0_{1s} = 100\,m/s$, $E_{1s}/R=15\,000\cdot T$; $b^0_{O_2} = 10^{-9}\,m^3/mol$; $q_{O_2}/R=10\,000\cdot T$, $k_{2s}=k_{3s}=k_{4s}=10^{-4}$ m/s.

For the reactions (2s)–(4s) the more simple rate equations were used:

$$r_i = k_{is} C_i \cdot (S/V).$$

In order to estimate the permissible values of the rate constants of each heterogeneous step, the pre-exponential factor values, k_0, presented in [14] for the similar types of heterogeneous reactions, were used.

The residence time dependencies of the reagent conversion, selectivity and yield of C_2 hydrocarbons are shown in Fig. 4. As seen from Figs. 1 and 4, the introduction of the heterogeneous steps into reaction mechanism results in increase of ethane+ethylene selectivity and yield in comparison to homogeneous reaction. The effect is significant: maximum yield of

Table 3
Results of computer simulations for the homogeneous–heterogeneous OCM reaction

T (K)	P (MPa)	Conversion (%)		Selectivity (%)						Y_{C_2} (%)
		CH_4	O_2	C_2H_4	C_2H_6	C_2^+	CO	CO_2	C_2H_2	
823	0.20	39.00	64.47	28.73	16.70	45.43	43.30	3.16	8.07	17.72
823	0.30	43.35	79.04	25.59	12.20	37.79	47.57	5.17	9.44	16.38
823	0.35	44.58	84.02	24.31	10.97	35.28	48.76	6.05	9.89	15.73
823	0.40	45.45	87.95	23.22	10.06	33.28	49.62	6.83	10.25	15.13
823	0.50	46.40	93.50	21.47	8.80	30.28	50.75	8.16	10.79	14.05
823	0.60	46.69	96.93	20.14	7.94	28.078	51.50	9.25	11.16	13.11
723	0.35	14.78	30.87	4.52	12.13	16.66	81.22	1.915	0.137	2.46
748	0.35	22.06	44.85	9.40	14.47	23.88	72.65	2.79	0.624	5.27
773	0.35	29.72	58.43	15.55	14.98	30.53	63.70	3.69	2.03	9.08
798	0.35	37.33	71.42	21.14	13.50	34.64	55.59	4.74	5.00	12.93
823	0.35	44.58	84.02	24.31	10.97	35.28	48.76	6.05	9.89	15.73
848	0.35	50.51	94.80	24.56	8.37	32.93	43.11	7.60	16.34	16.63
873	0.35	52.99	100.0	23.56	6.38	29.94	38.93	9.10	22.02	15.87

Inlet reaction mixture: 48% CH_4, 18% O_2, 34% H_2O, residence time; 10 s, ratio of surface area to reactor volume: $10^6\ m^{-1}$, Kinetic parameters for heterogeneous steps: $k_{1s}^0 = 100\ m/s$, $E_{1s}/R = 15\,000$ T; $b_{O2}^0 = 10^{-9}\ m^3/mol$; $q_{O_2}/R = 10\,000$ T, $k_{2s}=k_{3s}=k_{4s}=10^{-4}$ m/s.

C_2 hydrocarbons increases from 3.83% for homogeneous reaction to 16.24% for heterogeneous–homogeneous catalysis.

Comparisons of the results presented in Tables 1 and 3 show that there is a certain accordance between experimental and calculated data with respect to the levels of conversions, selectivity and yield as well as the tendency of their change with change of temperature and pressure. This indicates that the supposed kinetic model of the OCM reaction reflects some principal features of the heterogeneous–homogeneous OCM reaction under considered conditions.

Other important factor is the ratio of surface area to free reactor volume. Indeed, the S/V ratio influences the yield of C_2 hydrocarbons at given rate constants of heterogeneous reactions and residence time (Fig. 5).

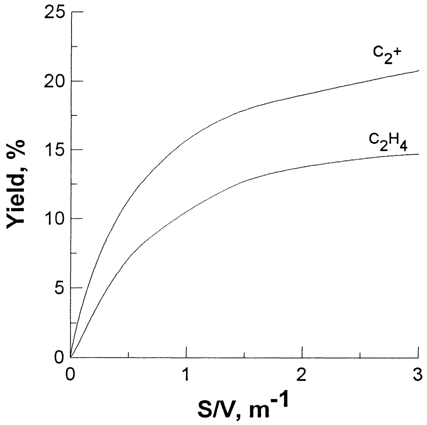

Fig. 5. Dependence of yield of C_2 hydrocarbons and ethylene on S/V ratio for the operating conditions on Fig. 4.

5. Conclusions

The results of the computer simulations show that a heterogeneous catalyst can efficiently control the reaction selectivity and yield of C_2 hydrocarbons for the low-temperature methane oxidative coupling at elevated pressures. Thus, one may hope for a success in improving the efficiency of the OCM reaction, efficiency by change of the catalyst properties and the surface area/volume reactor organization.

References

[1] N.I. Ilchenko, L.N. Rayevskaya, A.I. Bostan, G.I. Golodets, Kinet. Catal. 32 (1991) 873.

[2] N.I. Ilchenko, Yu.I. Pyatnitsky, in: S.T. Oyama (Ed.), The Chemistry of Transition Metal Carbides and Nitrides, Chap. 16, Blackie Academic and Professional, London, 1996, p. 311.

[3] N.I. Ilchenko, Yu.I. Pyatnitsky, Abstracts of the Second Workshop Meeting "C_1–C_3 Hydrocarbon Conversion", Krasnoyarsk, Russia, June 1994, p. 18.

[4] N.I. Ilchenko, N.V. Pavlenko, V.D. Pokhodenko, Yu.I. Pyatnitsky, T.H. Fleish, T.P. Kobylinski, C. Udovich, Abstracts of the 11th International Congress on Catalysis, Baltimore, July 1996, Rice University Printing Center, 1996, p. 256.
[5] H. Zanthoff, Z. Zhang, T. Grzybek, L. Lehman, M. Baerns, Catal. Today 13 (1992) 469.
[6] J.W.M.H. Geerts, Q. Chen, J.M.N. Van Kasteren, K. Van Der Wiele, Catal. Today 6 (1990) 519.
[7] J.Y. Zhu, R. Dittmayer, H. Hoffman, Chem. Eng. Process 32 (1993) 167.
[8] C.A. Mims, R. Mauti, A.M. Dean, K.D. Rose, J. Phys. Chem. 98 (1994) 13357.
[9] M.Yu. Sinev, Catal. Today 24 (1995) 389.
[10] J.A. Labinger, K.C. Ott, J. Phys. Chem. 91 (1987) 2682.
[11] G.J. Tjatjopoulos, I.A. Vasalos, Appl. Catal. A 88 (1992) 213.
[12] W. Tsang, R.F. Hampson, J. Phys. Chem. Ref. Data 15 (1986) 1087.
[13] P. Borrell, C.J. Cobos, A.E. Crose de Cobos, H. Hippler, K. Luther, A.R. Ravishankara, J. Troe, Ber. Bunsenges. Phys. Chem. 89 (1985) 337.
[14] O.V. Krylov, M.U. Kislyuk, B.R. Shub, A.A. Gezalov, N.D. Maksimova, Yu.N. Rufov, Kinet. Catal. 13 (1972) 598.